SCIENCE CHINA
Earth Sciences

•RESEARCH PAPER•

July 2018 Vol.61 No.7: 940–950
https://doi.org/10.1007/s11430-017-9169-4

Impact of anthropogenic drivers on subaqueous topographical change in the Datong to Xuliujing reach of the Yangtze River

Shuwei ZHENG[1], Heqin CHENG[1*], Shengyu SHI[1], Wei XU[1], Quanping ZHOU[2], Yuehua JIANG[2], Fengnian ZHOU[3] & Minxiong CAO[4]

[1] *State Key Laboratory of Estuarine and Coastal Research, East China Normal University, Shanghai 200062, China;*
[2] *Nanjing Geological Survey Center, China Geological Survey, Nanjing 210016, China;*
[3] *Yangtze River Water Resources Commission, Yangtze River Hydrology and Water Resources Survey Bureau, Shanghai 200136, China;*
[4] *Nanjing Hydraulic Research Institute, State Key Laboratory of Hydrology-Water Resources and Hydraulic Engineering, Nanjing 210098, China*

Received July 6, 2017; revised December 7, 2017; accepted January 24, 2018; published online April 12, 2018

Abstract Changes of subaqueous topography in shallow offshore water pose safety risks for embankments, navigation, and ports. This study conducted measurements of subaqueous topography between Datong and Xuliujing in the Yangtze River using a SeaBat 7125 multi-beam echo sounder, and the channel change from 1998 to 2013 was calculated using historical bathymetry data. The study revealed several important results: (1) the overall pattern of changes through the studied stretch of the river was erosion–deposition–erosion. Erosion with a volume 700×10^6 m^3 occurred in the upper reach, deposition of about 204×10^6 m^3 occurred in the middle reach, and erosion of about 602×10^6 m^3 occurred in the lower reach. (2) Dunes are the most common microtopographic feature, accounting for 64.3% of the Datong to Xuliujing reach, followed by erosional topography and flat river topography, accounting for 27.6% and 6.6%, respectively. (3) Human activities have a direct impact on the development of the microtopography. For instance, the mining of sand formed holes on the surface of dunes with lengths of 20–35 m and depths of 3–5 m. We concluded that the overall trend of erosion (net erosion volume of 468×10^6 m^3) occurred in the study area mainly because of the decreased sediment discharge following the closure of the Three Gorges Dam. However, other human activities were also impact factors of topographic change. Use of embankments and channel management reduced channel width, restricted river meandering, and exacerbated the erosion phenomenon.

Keywords Subaqueous topographical, Human activities, Multi-beam echo sounder, High resolution, Yangtze River

Citation: Zheng S W, Cheng H Q, Shi S Y, Xu W, Zhou Q P, Jiang Y H, Zhou F N, Cao M X. 2018. Impact of anthropogenic drivers on subaqueous topographical change in the Datong to Xuliujing reach of the Yangtze River. Science China Earth Sciences, 61: 940–950, https://doi.org/10.1007/s11430-017-9169-4

1. Introduction

Subaqueous topography is a collective term for various bedforms in rivers, lakes, and oceans, and the size, morphology, and evolution mechanisms of the topography are related closely to the sedimentary environment (Wu et al., 2014; Wu Z Y et al., 2016; Zheng et al., 2016; Schindler et al., 2015) and important for the safety of embankments, navigation, and ports (Knaapen, 2005). As a result, the study of subaqueous topography is gaining increasing importance in geography and engineering.

The complex dynamic sedimentary environment of the Yangtze River (YR) has formed a great variety of subaqueous topographies in the river channels and estuary. Previous scholars have performed a series of studies using field surveying, GIS technology, and historical data (Chen et al.,

* Corresponding author (email: hqch@sklec.ecnu.edu.cn)

1986; Song and Wang, 2014; Chen et al., 1993; Wu et al., 2009). Chen et al. (1959) summarized the development model of the YR estuary using shallow and deep borings and historical data. Qu (2014) analyzed the channel change using GIS technology. Many scholars, using side scan sonar and sub-bottom profiler methods, have studied the development mechanism of the dunes (Wang Z et al., 2007; Chen et al., 2012; Wu et al., 2009). Some studies have taken a typical reach of the river as an example and studied the relationships between water and sediment discharges and channel changes (Li et al., 2015). These studies have greatly increased our understanding of the evolution of the subaqueous topography. However, due to improvements in research technology, the fine structures and evolution mechanisms of microtopography have attracted increasing attention (Knaapen et al., 2001; Best, 2005; Barnard et al., 2011; Franzetti et al., 2013; Perillo et al., 2014). Nevertheless, understandings of the relationships between the development of microtopography and topographic evolution at the channel scale because of human intervention are still limited.

Highly utilized in navigation and having abundant embankments, the segment of the YR from Datong to Xuliujing is greatly affected by human activities. However, due to the lack of high-resolution bathymetric data, understandings of the multi-scale subaqueous topography are still evolving and need to be enhanced. Therefore, this study examined the subaqueous topography of this part of the YR at different scales using high-resolution, multi-beam data and GIS technology. The objectives of the study were to determine: (1) the trends of deposition and erosion in the reach between Datong and Xuliujing from 1998 to 2013, and (2) how the Three Gorges Dams (TGD), embankments, and navigation management have influenced the subaqueous topography at multi-scales.

2. Regional setting and methods

2.1 Regional setting

With a length of 6300 km and drainage area of 1.81×10^6 m^2, the Yangtze River is the longest river in China. Precipitation in the YR basin is abundant in the flood season from May to October and is concentrated mainly in July to August (Wang J et al., 2007). The maximum runoff, recorded at Datong Station, is 92600 m^3 s^{-1} (Aug. 1954), and the minimum value is 4620 m^3 s^{-1}. The average sediment discharge and average median grain size before the closure of the TGD (1990–2002) were 327×10^6 t and 0.009 mm, respectively (Xu, 2013). However, the sediment discharge has shown a significant declining trend since 2003 (Li et al., 2015; Yang et al., 2014). Statistical data show that the average sediment discharge from 2006–2010 is 130×10^6 t (http://www.cjw.gov.cn). Additionally, the patterns of deposition and erosion in the middle and lower YR have changed obviously. Overall channel erosion has extended gradually to Datong (Xu, 2013). In recent years, many projects have been constructed in the Datong–Xuliujing reach (e.g., Shuangjian shoal protection engineering projects). These projects have not only changed the water boundary conditions of the local river segment, but also have had a profound influence on the evolution of the subaqueous topography.

2.2 Methods

Bathymetry data (1:40000 scale) from Datong to Xuliujing in 1998 and 2013 were collected to investigate the channel changes. The bathymetric data were georeferenced in ArcGIS 10 software and the kriging method was used to create digital elevation models (DEMs). Then, volume changes were calculated between 1998 and 2013 based on these DEMs.

The subaqueous microtopography between Datong and Xuliujing in the YR was investigated using a Reson SeaBat 7125 multi-beam system during October 2014 and July and August 2015. This multi-beam system has an operational frequency of 200 or 400 kHz, and the maximum ping rate is 50±1 Hz. It has 512 beams at the frequency of 400 kHz with a central beam angle of 0.5°, and the highest depth resolution is 6 mm. The coverage width of the multi-beam data changes with water depth and instrument settings; for instance, the maximum coverage width is 5–6 times the water depth in the equidistant model, i.e., the coverage width is approximately 100 m when the water depth is 20 m. By using a Trimble real-time differential global positioning system (DGPS), decimeter-scale positional accuracy was achieved. The final grid model was created from the multi-beam point cloud data. All of the points were processed by roll, pitch, and yaw calibration and abnormal beam removal. In this study, we statistically analyzed the microtopography along the main navigated waterway downstream of Datong (approximately 560 km long). A ~68 km long reach within the waterway was not involved in the final result because the survey line deviated from the main navigated waterway.

A dual frequency acoustic doppler current profiler (ADCP, Rowe Technologies Inc.) was used to collect flow velocity data. It has a working frequency of 300 and 600 kHz with a measuring range of ±5 m s^{-1}. This instrument was fixed onto a custom-made shelf during the survey. In this survey, the ADCP data included 10, 9, 17, 11, and 23 h of flow velocity data from five short-term stations, respectively (Figure 1).

Bed surface sediments were sampled along the main navigation channel at each 10 km with a sediment sampler that could sample a 3–10 cm layer of the riverbed (Zheng et al., 2017). In total, 21 samples were collected in the study area (Figure 1). The grain size of the sediments was analyzed in the laboratory by using a Mastersizer 2000 laser analyzer

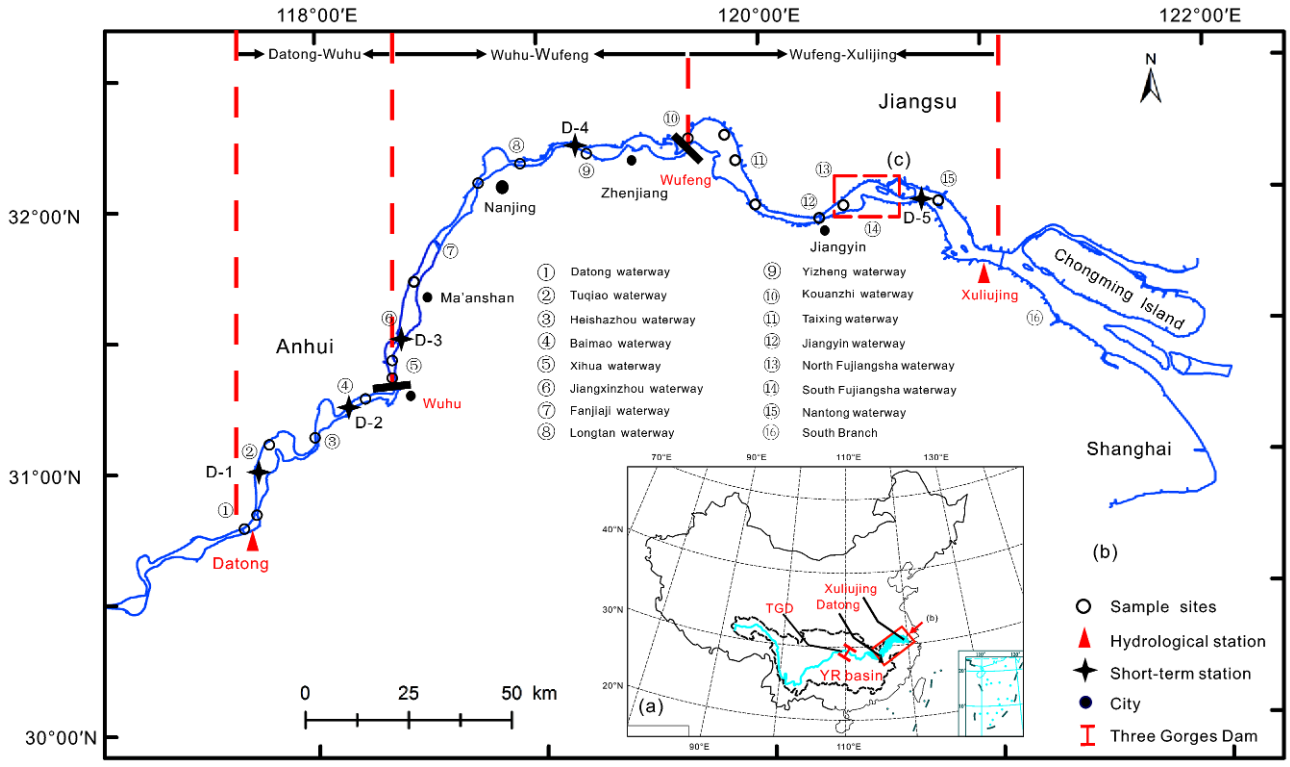

Figure 1 Map of the study area showing the Yangtze River basin. (a) The Yangtze River basin; (b) the sample sites and short-term station locations.

(Malvern Instruments, UK). The process was as follows: obtain suitable samples and place them into a beaker, use 10% H_2O_2 and 10% HCl to remove organic matter and $CaCO_3$ concretions, respectively, then add $(Na_2PO_3)_6$ to disperse the sample. Several samples that included gravel were analyzed using a Camsizer XT (Retsch Technology, Germany; Table 1). The B-CCD and Z-CCD camera with a measurement range of 0.001–30 mm was used to record the grain size and morphology (Luo et al., 2016). In this study, the dry method (X-FALL) was chosen to analyze the samples.

3. Results

3.1 Bed material characteristics

Most of the riverbed sediment in the reach between Datong and Xuliujing is sandy (>63 μm). The median grain size ranged from 68.2–273.0 μm (Table 1). There is a mud layer with a thickness of 1–3 cm between the Yizheng waterway and the Kouanzhi waterway (median grain size of 11.2–13.2 μm), and the median grain size of the sediment below this mud layer is 253.7–270.0 μm.

3.2 Flow velocity characteristics of the short-term stations

There are five short-term stations in the dune area. Four of these stations are influenced mainly by runoff and have a mean flow velocity of 0.67–0.99 m s^{-1}. One station is influenced by bidirectional flow, and the maximum flow velocities in flood and ebb tide are 0.88 m s^{-1} and 1.03 m s^{-1}, respectively (Table 2).

3.3 Channel change trend between Datong and Xuliujing

Overall, the net erosion volume between Datong and Xuliujing from 1998 to 2013 was 468×10^6 m^3. However, there was an "erosion-deposition-erosion" pattern from Datong to Xuliujing. Thus, we divided the study reach into the Datong-Wuhu, Wuhu-Wufeng, and Wufeng-Xuliujing reaches. The erosion volume in the Datong-Wuhu reach was 70×10^6 m^3, the deposition in the Wuhu-Wufeng reach was about 204×10^6 m^3, and the erosion in the Wufeng–Xuliujing reach was about 602×10^6 m^3 (Table 3). The specific features of these reaches are described below:

(1) The Datong–Wuhu reach mainly incurred erosion with an annual intensity of 38.9×10^3 m^3 km^{-1}. Overall, the erosion occurred mainly in the water depths of 2–10 m. Depths of 0–2 m incurred slight siltation, and those below 10 m were stable (Table 3). This phenomenon suggests that the 2–10 m riverbed responded sensitively to the sediment decline. The analysis also showed that although most parts of the Datong–

Table 1 Grain size parameters of the surface sediment between Datong and Xuliujing in the Yangtze River[a)]

Location	Distance from Datong (km)	Kinetic (Φ)	Sorting coefficient (Φ)	Skewness (Φ)	Number of peak	Median grain size (μm)	Depth (m)
Datong waterway	0	3.23	0.34	0.51	single	249.0	–
Tuqiao waterway	10	3.07	1.97	0.79	single	121.8	13
Tuqiao waterway	40	3.39	1.32	0.48	single	211.1	25
South heishazhou waterway	70	3.59	1.28	0.50	single	245.7	10
Baimao waerway	100	0.98	2.18	0.70	single	95.3	19
Xihua waterway	120	3.94	1.59	0.71	single	273.4	11
Jiangxinzhou waterway	130	3.47	1.96	0.78	single	152.7	13
Fanjiaji waterway	160	3.48	1.37	0.55	single	233.9	11
Longtan waterway	220	3.456	1.23	0.49	single	193.7	14
Longtan waterway	230	3.04	1.87	0.73	single	159.8	30
Yizheng waterway[a)]	270	1.28	2.23	0.01	single	13.2	14
Yizheng waterway[b)]	270	–	–	–	single	269.9	14
Kouanzhi waterway[a)]	320	1.02	1.67	0.26	single	11.2	20
Kouanzhi waterway[b)]	320	–	–	–	single	253.7	20
Kouanzhi waterway	340	3.40	1.48	0.64	single	170.1	22
Taixing waterway	357	2.35	1.64	0.55	double	261.0	19
Jiangyin waterway	380	3.65	1.68	0.62	double	261.6	14
Jiangyin waterway	405	2.57	1.76	0.19	double	235.8	–
North Fujiangsha waterway	410	0.98	2.09	0.72	single	182.3	7
South Fujiangsha waterway	420	3.62	1.76	0.73	single	136.8	–
Nantong waterway	450	3.64	1.24	0.57	single	68.2	–
Baimaosha waterway	480	0.99	2.50	0.09	double	18.5	–

a) The distance from Datong is positive in the downstream direction. "–" means no data. The samples in the Yizheng waterway and the Kouanzhi waterway were analyzed using a Camsizer XT; there were no kinetic, sorting coefficient, or skewness data for these samples. The mean real-time water depth when sampling is indicated. *, sediment samples of the 1–3 cm mud layer, **, sediment beneath the mud layer.

Table 2 The flow velocity characteristics in the short-term stations between Datong and Xuliujing[a)]

Locations	Mean velocity ($m\ s^{-1}$)	Start time	End time	Observation time (h)	Discharge ($m^3\ s^{-1}$)	Froude number	Depth (m)
D-1	0.99	2015.08.03	19:30	10	41500	0.07	17.6
D-2	0.91	2015.08.10	19:00	9	33500	0.09	10.4
D-3	0.78	2015.08.11	14:00	17	32500	0.08	10
D-4	0.67	2015.08.12	19:00	11	31800	0.07	11
D-5	V_1=1.03; V_2=0.88	2015.08.13	19:00	23	31200	0.05	14.9

a) V_1, the maximum flow velocity in ebb tide; V_2, the maximum flow velocity in flood tide.

Wuhu segment incurred scouring, the segment between Tianranzhou and Wuhu showed erosion followed by deposition (Figure 2b). Thus, we infer that this segment is in the process of adjusting and adapting to the reduction of sediment discharges.

(2) The channel change from Wuhu to Wufeng was complex, but the overall trend was a slight deposition. For instance, there was no obvious change from the Nanjing waterway to the Yizheng waterway, but the heads of the Bagua, Shiye, and Hechang sandbars showed obvious erosions and the other segments, e.g., the Jiaoshan waterway, showed depositions (Figure 2c). In addition, it is noteworthy that some segments of the surface sediments had a 1–3 cm mud layer on the top of the sandy riverbed, which may have been related to seasonal flood depositions.

(3) Overall, the Wufeng-Xuliujing segment show an erosion trend with an annual erosion intensity of $223\times10^3\ m^3\ km^{-1}$. For example, obvious erosion occurred from the Nantong waterway to the East Tongzhousha waterway (Figure 2d). In this segment, the water depths of 0–5 m and

Table 3 The channel change characteristics and statistical parameters of the Datong to Xuliujing segment in the Yangtze River (1998–2013)[a)]

Segment	Year	Shoreline envelope area ($\times10^6$ m^2)	Channel volume ($\times10^6$ m^3)	0–2 m channel volume ($\times10^6$ m^3)	2–5 m channel volume ($\times10^6$ m^3)	5–10 m channel volume ($\times10^6$ m^3)	Below 10 m channel volume ($\times10^6$ m^3)
Datong-Wuhu (120 km)	1998	252	1360	416	452	420	72
	2013	220	1430	403	489	468	69
	Difference	32	70	–13	37	48	–2
Wuhu-Wufeng (200 km)	1998	480	3228	801	986	531	910
	2013	450	3025	775	975	1072	202
	Difference	30	–204	–25	–11	540	–708
Wufeng-Xulijing (180 km)	1998	1096	5652	1233	1546	1984	889
	2013	818	6254	1471	1754	1760	1269
	Difference	278	602	239	207	–224	380

a) Positive values mean erosion or decline and negative values mean deposition or increase in the difference.

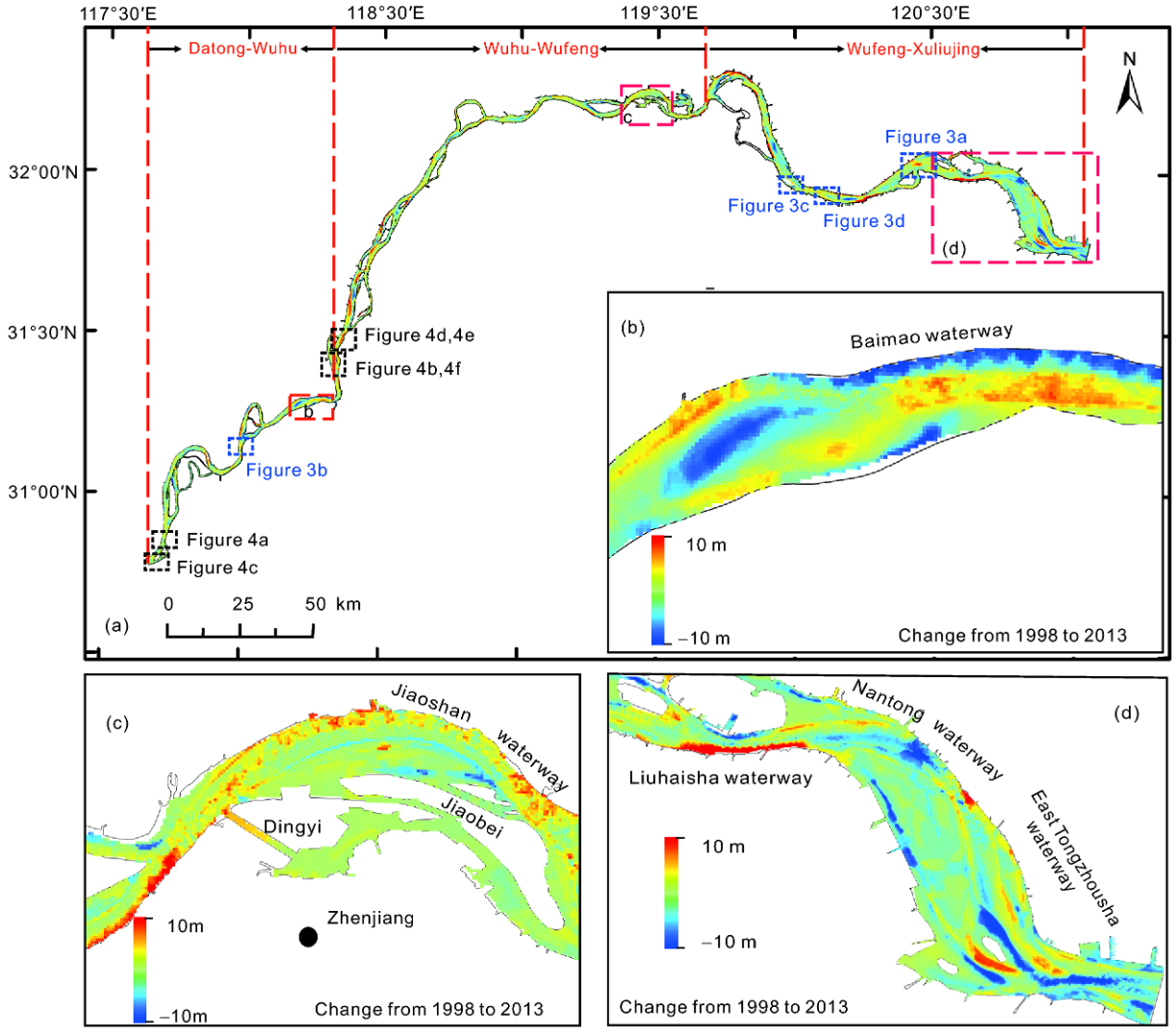

Figure 2 Maps showing the patterns of erosion and deposition between Datong and Xuliujing (1998–2013). (a) The erosion and deposition pattern between Datong and Xuliujing and the locations of the multi-beam data in Figures 3 and 4; (b) the phenomenon of erosion followed by deposition in the Baimao waterway. (c) the situation of deposition in the Jiaoshan waterway; (d) the entire riverbed erosion between the Nantong waterway and the East Tongzhousha waterway.

deeper than 10 m showed excess erosion, but the water depths between 5 m and 10 m incurred deposition. This phenomenon suggests that the 0–5 m and deeper than 10 m areas were the main areas of adjustment due to the reduction of sediment discharges.

3.4 Fine structure and morphology parameters of the microtopography

The statistical data showed that dune was the most widely developed riverbed microtopography downstream of Datong, accounting for 64.3% of the whole study reach, followed by erosional topography, such as erosional flutes and holes, accounting for 27.6% of the study reach. Flat riverbed accounted for 6.6% of the reach, and other composite topographies accounted for about 1.5%. The specific statistical results are described below:

(1) According to dune length (Ashley, 1990), the dunes can be classified into small size (length < 5 m), medium size (length 5–10 m), large size (length 10–100 m), and very large size (length > 10 m) dunes. Small and medium dunes accounted for 71.5% of the dunes in the study area, and large and very large dunes accounted for approximately 28.5% of the dunes (Figure 3a and 3b).

(2) Composite topography was one of the widely developed topographies downstream from Datong. It consists of a complex morphology characterized by superposition of two or more types of microtopography. It was mainly developed in the rapid topographical change area. One example of this microtopography is seasonal dunes superimposed on erosional holes (Figure 3d). Human activities also can form composite topography, e.g., holes from the mining of sand developed on dunes (Figure 4d).

(3) The diameter of a single sand mining hole ranged from 20 to 50 m and the depth ranged from 1.9 to 2.2 m. The volume of a single hole ranged from 5×10^3–19×10^3 m^3 (Table 4). This type of topography is usually formed by illegal sand mining, which is common on both sides of the main channel (Figure 4d). Some of these holes are only 50 m from the foot of the bank. Flat riverbed is a type of topography with a smooth or slightly undulating form. It is developed widely downstream of Jiangyin, but it is rarely observed upstream of Jiangyin.

(4) The cross-sectional morphology of the erosional flutes is nearly a "V" shape, and the flutes extend longitudinally as a strip-shaped groove. This type of topography is widely observed in narrow channel or at a side of the mainstream along scoured bank (Figure 4c). Taking the Yizheng waterway as an example, there is an erosional flute with a length of ~230 m developed in the right main navigation channel. Statistical data of the 282-m long flute (limited by navigation conditions; we could not observe the entire erosional flute) show a mean depth of erosion of 3.8 m and a volume of 131×10^3 m^3 (Table 4). Additionally, mainstream scouring at the

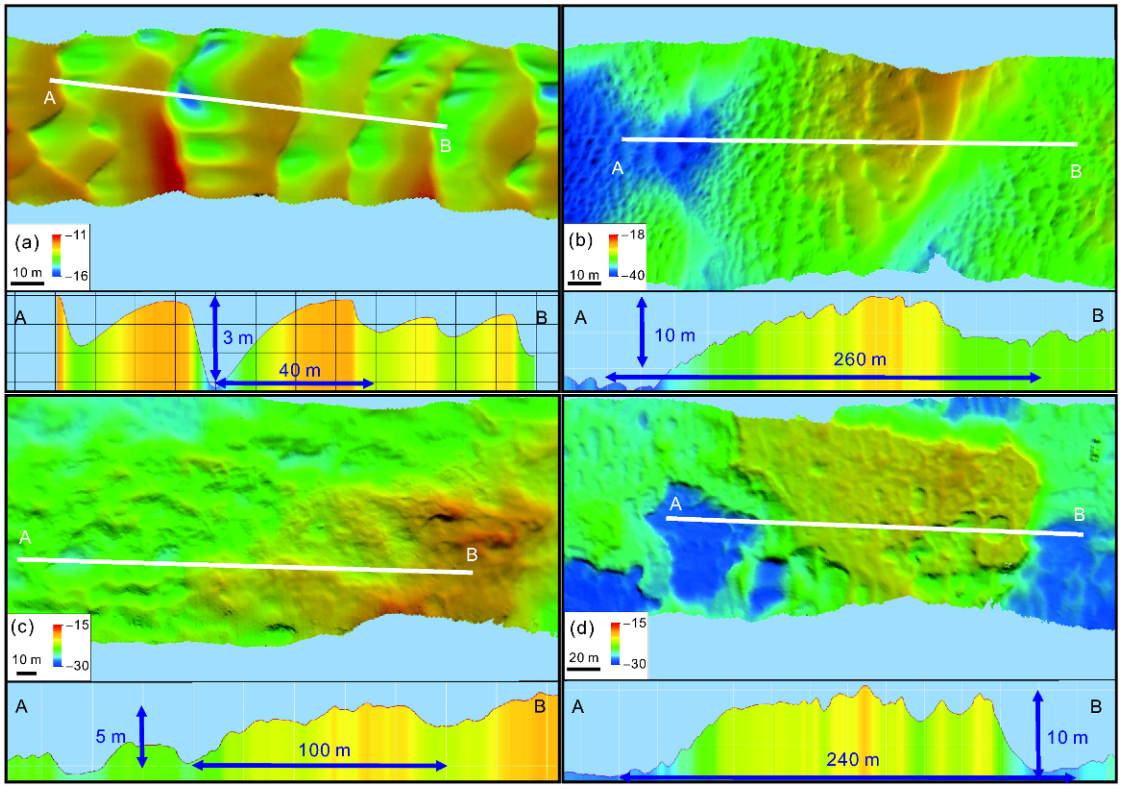

Figure 3 Maps showing the microtopography in the Yangtze River between Datong and Xuliujing (grid resolution of 0.5 m×0.5 m). (a) Large dunes, (b) very large dunes, (c) complex topography, (d) composite topography.

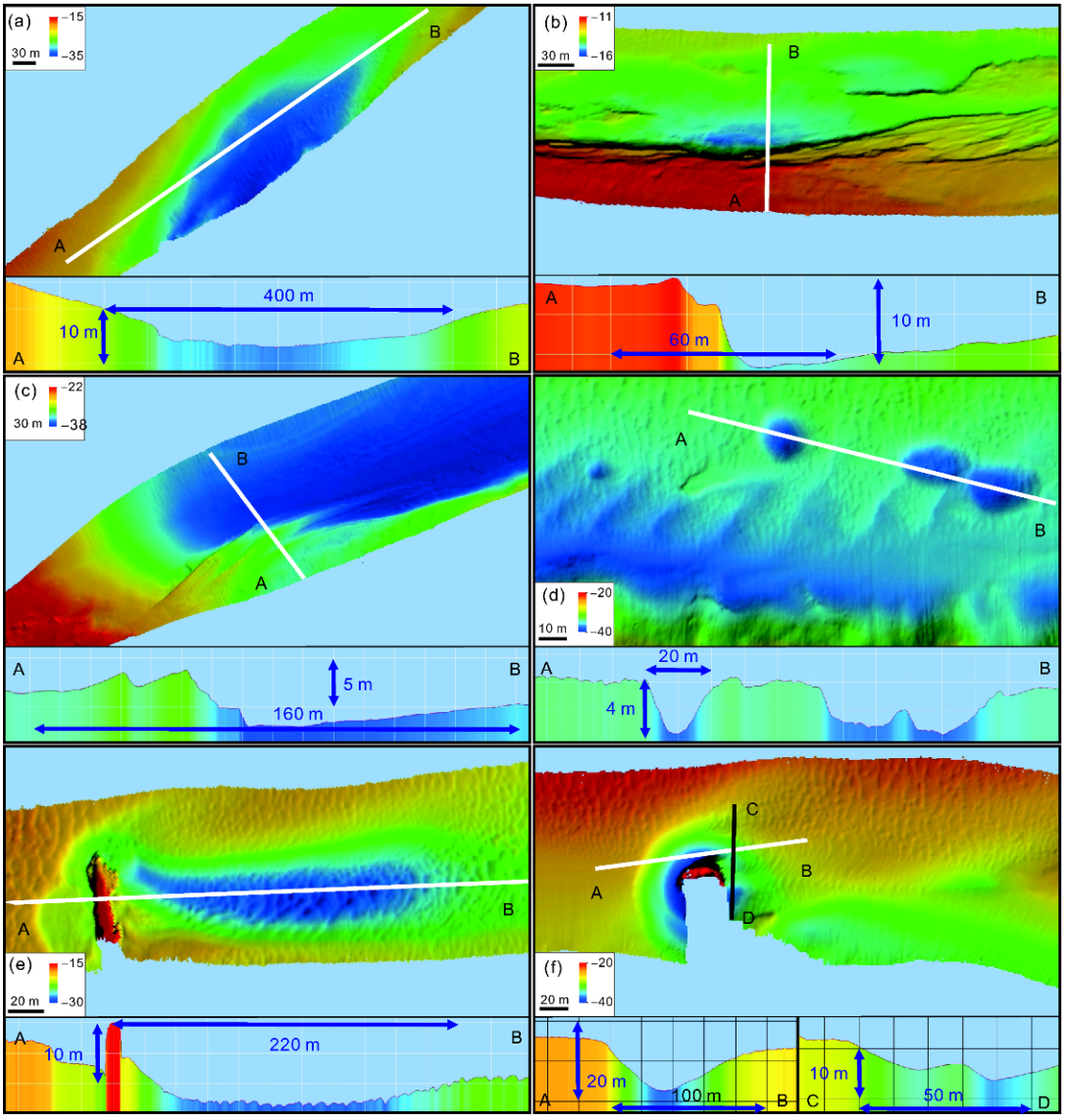

Figure 4 Micro-erosional topography developed in the Yangtze River between Datong and Xuliujing (grid resolution of 0.5 m×0.5 m). (a) Erosional holes, (b) scoured riverbank, (c) erosional flutes, (d) holes from sand mining, (e) erosional topography around sunken boats, (f) scour from the Wuhu Yangtze River Bridge.

foot of the riverbank formed a slope ratio of more than 1:2 in some segments. This type of topography is developed widely along the main navigation channel near the riverbank (Figure 4b). Erosional holes are also commonly observed in the channel. This microtopography has the form of an oval-shaped or irregular pit within a small area with the characteristic of sudden depth change (Figure 4a). As an example, an erosional hole with a size of 122 m×226 m was observed in the Yizheng waterway. It was about 2.9 m deeper than the surrounding riverbed and had a volume of 112×10^3 m^3 (Table 4).

In addition, local erosional or depositional phenomena can be caused by artificial structures, e.g., sunken boats or bridge foundations (Figure 4e and 4f). A sunken boat with a length of 20–40 m may cause erosion of 48×10^3 m^3 of sediment from the riverbed. The erosional topography in the downstream of sunken boat had a mean depth of 2.8 m and mean length of 287 m (Figure 4e). Statistical data of several bridge foundations in the YR showed that a bridge foundation can cause riverbed scouring with a volume of 66×10^3–181×10^3 m^3. Examples include the Second Nanjing Yangtze River Bridge, the Dashengguan Yangtze River Bridge, and the Tongling Yangtze River Bridge (Table 4).

4. Discussion

4.1 Impacts of the Three Gorges Dam on the subaqueous topography change

Changes in subaqueous topography of the river channel are the result of flow, sediment, and riverbed morphology. Therefore, the river channel change is closely related to

changes of flow and sediment discharge in the upper reaches (Xu, 2013; Yang et al., 2015). The sediment discharge showed a decline trend after the closure of the TGD (Figure 5). Statistical data at Datong showed that the suspended sediment discharge (SSD) and suspended sediment content (SSC) were 4.33×10^9 t and 0.486 kg m^{-3} during 1950–2000, respectively. However, the SSD and SSC decreased to 1.39×10^9 t and 0.162 kg m^{-3} in 2003–2015, respectively (http://www.cjw.gov.cn). The substantial declines of SSD and SSC in the YR basin have enhanced the sediment-carrying capacity of the flow discharge and have led to erosion of sediment from riverbed (Qian and Wang, 2003). Thus, a large amount of sediment was trapped in the upstream reaches of the YR because of the dams and reservoirs. Moreover, the obvious declines of SSD and SSC are the main reason for the 468×10^6 m^3 of sediment erosion from the riverbed in the study area. This finding is consistent with the results of many other scholars. The channel of the middle and lower YR has changed to adjust to the decreased sediment discharges following the impoundment of the TGD in 2003, and several reaches have incurred excess erosion (Yang et al., 2011). For instance, Xia et al. (2016) concluded that operation of the TGD is the direct reason for the decline in sediment discharges in the Jingjiang reach; SSC also decreased from 1.35 (1956–2002) to 0.28 kg m^{-3} (2002–2013). As a result, the total volume of erosion in the Jingjiang reach was as much as 700×10^6 t. Luo et al. (2017) found that human activities including the operation of the TGD have led to a dramatic decline of sediment supply in the YR delta. Although some of the subaqueous topography remains depositional, the entire delta is experiencing a process of net erosion and the riverbed sediment is coarse.

4.2 Impacts of other human activities on the subaqueous topographical changes

4.2.1 Sand mining

Sand mining in the main channel of the YR was banned in 2000, which changed the disordered and chaotic situation of sand mining. However, illegal sand mining occurs from time to time. For instance, the volume of illegal sand mining at Langshansha in the Xuliujing reach was approximately 7.8×10^6 m^3 during 2011–2012 (Liu et al., 2014). The multi-beam data showed that illegal sand mining holes are usually distributed on the margin of the navigation channel. However, some sand mining holes, with a maximum diameter of 50 m and maximum volume of 19×10^3 m^3, were only 50 m from the foot of the riverbanks (Figure 4d). Illegal sand mining activity influences sediment transport and changes the morphology of the microtopography. More importantly, sand mining can disturb the flow structure and lead to riverbed deformation. Therefore, the volume and locations of the sand mining are of significance to subaqueous topographical changes. A study showed that the volume of sand mining in the Xuliujing reach was 120×10^6 m^3 during 2003–2010 (Liu et al., 2014). However, the total volume of erosion between Jiangyin and Xuliujing was 322.5×10^6 m^3 during 1998–2013. Hence, the cumulative effect of sand mining cannot be disregarded.

4.2.2 Bridge foundations

Artificial structures (e.g., bridge foundations) can change flow structure and lead to deformation of subaqueous topography. Several bridges have been built across the Yangtze River between Datong and Xuliujing since 1964. Although the bridge foundations differ in size, shape, and type and the sedimentary environment surrounding each foundation is typically different, the multi-beam data showed that the riverbed surrounding these foundations experienced erosion of various degrees (Table 4). For example, an erosional hole with a length of ~390 m and erosion volume of 181×10^3 m^3 was observed surrounding the main foundation of the Second Nanjing Yangtze River Bridge (YRB). Previous studies have indicated that bridge foundations can lead to severe erosion of the local riverbed. Additionally, the bridge foundation narrowed the channel, which resulted in whole riverbed erosion, coarser sediment, and a change in the symmetry feature of dunes (Lu, 2016; Guo et al., 2015). Our multi-beam data between Datong and Jiangyin showed that the subaqueous topography surrounding bridge foundation was dominated by erosional topography. For instance, erosional topography with the shape of a “C” and with a length greater

Table 4 Statistical parameters of microtopography in the Yangtze River from Datong to Xuliujing

Topography	Erosion area ($\times10^3$ m^2)	Erosion volume ($\times10^3$ m^3)	Erosion depth (m)	Length (m)	Width (m)
The second Nanjing YRB	59	181	3.0	390	169
The Dashengguan YRB	44	108	2.4	256	95
The Tongling YRB	43	66	1.5	196	306
Erosional holes	39	112	2.9	226	112
Erosional flutes	35	131	3.8	282	232
Sinking boat	17	48	2.8	287	60
Sand mining holes	3–8	5–19	1.9–2.2	20–50	16–20

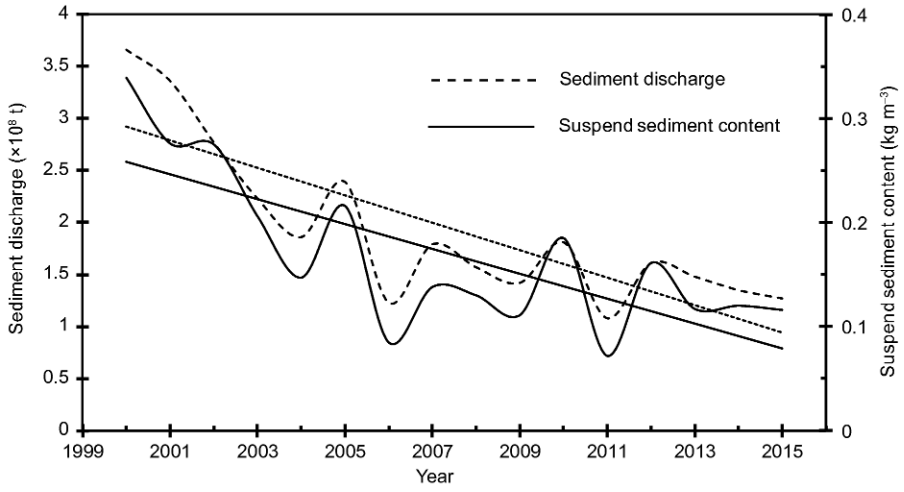

Figure 5 Change of annual sediment discharge and suspended sediment content at Datong station (2000–2015).

than 100 m and depth greater than 10 m was observed at the bridge foundation of the Wuhu YRB.

4.2.3 Channel regulations and development

Erosional topography developed on riverbed or in riverbanks is commonly observed in alluvial rivers, and human activities (e.g., channel governance) may influence the development of erosional topography (Zhong et al., 2005; Wu S H et al., 2016). Taking the Wufeng–Xuliujing reach as an example, the shoreline envelope area was reduced by ~278×10^6 m^2, which accounts for 25.4% of the total area in 1998, due to channel management, shoreline utilization, deposition promotion projects, and man-made acceleration of sand bars (Table 3). Channel management projects not only narrow the channel and fix the river boundaries, but also restrict the river meandering. This may lead to more serious bank erosion. As an example, there is an erosional flute with a length of more than several thousand meters in the channel-controlled segment of the Liuhaisha waterway and Tongzhousha waterway (Figure 2d). The multi-beam data suggested that erosional holes (Figure 4a) or erosional flutes (Figure 4c) were developed to depths of more than 10 m and lengths of more than 100 m in several channel segments between Datong and Xuliujing. Furthermore, the erosional banks can be eroded by more than 5 m within 10 m long (Figure 4b). Therefore, the impacts of channel management and shoreline utilization projects on the subaqueous topography cannot be neglected.

4.3 Relationship between channel change patterns and microtopography development

The development of small-scale topography is closely related to the formation of channel-scale topography. Thus, the movement of dunes can predict the stability of the channel (Wang W W et al., 2007). On the other hand, the evolution of channel-scale topography is also influenced by the development of small-scale topography. The construction of the Qingcaosha Reservoir in the North Channel of the YR estuary has narrowed the channel width and led to channel erosion from 2002 to 2012, which has increased the movement of bedload and could be beneficial to the development of small-scale topography (dunes) (Wu S H et al., 2016). The pattern of change of subaqueous topography between Datong and Xuliujing was upper reach erosion, middle reach deposition, and lower reach excessive erosion, under the influence of natural and human activities in 1998–2013. Except for the mud layer (median grain size range of 11.2–13.2 μm) observed in the middle reach area of deposition, the median grain size in other reaches ranged from 68.2 to 273.0 μm. This grain size result is similar to grain size results of previous studies, and it is a necessary condition for dune development (Zhuang et al., 2004). Meanwhile, the runoff showed a mean flow velocity of 0.67–0.99 m s^{-1}, and maximum velocity of bidirectional flow was 0.88 and 1.03 m s^{-1} for flood tide and ebb tide, respectively (Table 2). These flow conditions are also beneficial for the development of dunes (Cheng et al., 2002). Therefore, for the time being, the dynamic environment between Datong and Xuliujing is beneficial for the development of dunes.

5. Conclusions

High-resolution multi-beam data and GIS technology were used to analyze the characteristics and the changes of subaqueous topography between Datong and Xuliujing. The main findings of the study are:

(1) Overall, the change pattern of subaqueous topography in the Datong to Xuliujing reach during 1998–2013 was erosion-deposition-erosion. Erosion with a volume of 70×10^6 m^3 occurred in the Datong–Wuhu segment of the reach, deposition of about 204×10^6 m^3 occurred in the Wuhu–Wu-

feng segment, and erosion of about 602×10^6 m^3 occurred in the Wufeng-Xuliujing segment.

(2) Dunes are the common microtopography, accounting for 64.3% of the study reach, followed by erosional topography (approximately 27.6%, e.g., erosional flutes and holes) and flat river (6.6%). Among the dunes, small and medium dunes accounted for 71.5% of the bedforms and large and very large dunes accounted for approximately 28.5%.

(3) Human activities can have direct impacts on the development of microtopography. For instance, sand mining in the study area formed holes on the surface of dunes with a length of 20–35 m and depth of 3–5 m. Bridge foundations can form erosional topography with a length exceeding 100 m and a volume as large as 60×10^3–181×10^3 m^3. We concluded that the overall erosion trend between Datong and Xuliujing occurred mainly due to decreased sediment discharges following the closure of the Three Gorges Dam. Other human activities are also impact factors of topography change. Embankments and channel management can cause the channel width to shrink, restrict river meandering, and exacerbate erosional phenomena.

Acknowledgements *We thank the two reviewers for their insightful comments and contributions. Thanks go to Wu Shuaihu, Lu Xuejun, Luo Zhang, Cai Bing, Luo Zhifa, Zhan Jian, Dong Weili and Xu Houyong. This study was financially supported by the National Natural Science Foundation of China (Grant Nos. 51761135023 & 41476075) and the China Geological Survey (Grant No. DD20160246).*

References

Ashley G. M. 1990. Classification of large-scale subaqueous bed forms: A new look at an old problem. J Sediment Petrol, 1: 160–172
Best J. 2005. The fluid dynamics of river dunes: A review and some future research directions. J Geophys Res, 110: F04S02
Barnard P L, Erikson L H, Kvitek R G. 2011. Small-scale sediment transport patterns and bedform morphodynamics: New insights from high-resolution multibeam bathymetry. Geo-Mar Lett, 31: 227–236
Chen J, Wang Z B, Li M T, Wei T Y, Chen Z Y. 2012. Bedform characteristics during falling flood stage and morphodynamic interpretation of the middle-lower Changjiang (Yangtze) River channel, China. Geomorphology, 147-148: 18–26
Chen J Y, Yu Z Y, Yun C X. 1959. The development of the Yangtze River Delta (in Chinese). Acta Geogr Sin, 3: 201–220
Chen W M, Yang Z S, Cao L H, Guo Z G, Liu H, Du J P. 1993. Micro-geomorphology on the subaqueous slope of the Changjiang River Delta (in Chinese). J Ocean Univ Qingdao, S1: 45–51
Chen Z Y, Zhou C Z, Yang W D, Wu Z G. 1986. Subaqueous topography and sediments off modern Changjiang Estuary (in Chinese). Donghai Mar Sci, 2: 28–37
Cheng H Q, Li M T, Zhou T Y, Xue Y Z. 2002. High-resolution micro-topography movement in the Changjiang Estuary (in Chinese). China Ocean Eng, 20: 91–95
Franzetti M, Le Roy P, Delacourt C, Garlan T, Cancouët R, Sukhovich A, Deschamps A. 2013. Giant dune morphologies and dynamics in a deep continental shelf environment: Example of the banc du four (Western Brittany, France). Mar Geol, 346: 17–30
Guo X J, Cheng H Q, Mo R Y, Yang Z Y. 2015. Statistical characteristics and transport law of sand waves in the Yangtze Estuary (in Chinese). Haiyang Xuebao, 37: 148–158
Knaapen M A F. 2005. Sandwave migration predictor based on shape information. J Geophys Res, 110: F04S11
Knaapen M A F, Hulscher S J M H, de Vriend H J, Stolk A. 2001. A new type of sea bed waves. Geophys Res Lett, 28: 1323–1326
Li B, Yan X S, He Z F, Chen Y, Zhang J H. 2015. Impacts of the Three Gorges Dam on the bathymetric ecolution of the Yangtze River Estuary (in Chinese). Chin Sci Bull, 60: 1735–1744
Liu G P, Xu H, Bi J F. 2014. The analysis of sand mining and its influence to river channel evolution at Jiangsu segment in the Yangtze Estuary (in Chinese). Yangtze River, S2: 193–196
Lu X J. 2016. Research on the local scour at bridge piers in the tidal reach of the Changjiang River (in Chinese). Doctoral Dissertation. Shanghai: East China Normal University
Luo X X, Yang S L, Wang R S, Zhang C Y, Li P. 2017. New evidence of Yangtze delta recession after closing of the Three Gorges Dam. Sci Rep, 7: 41735
Luo Z, Cai B, Chen S L. 2016. Grain size and shape analysis of beach sediment using dynamic image analysis and comparison with sieving method (in Chinese). Acta Sediment Sin, 34: 881–891
Perillo M M, Best J L, Garcia M H. 2014. A new phase diagram for combined-flow bedforms. J Sediment Res, 84: 301–313
Qian N, Wang Z H. 2003. Mechanics of Sediment Movement (in Chinese).. Beijing: Science Press. 145–189
Qu G X. 2014. The characteristics and explanations of channel change in the Datong-Jiangyin reach of the lower Yangtze River: 1958–2008 (in Chinese). Doctoral Dissertation. Nanjing: Nanjing Normal University
Song C C, Wang J. 2014. Erosion-accretion changes and controlled factors of the submerged delta in the Yangtze Estuary in 1982–2010 (in Chinese). Acta Geol Sin, 11: 1683–1696
Schindler R J, Parsons D R, Ye L, Hope J A, Baas J H, Peakall J, Manning A J, Aspden R J, Malarkey J, Simmons S, Paterson D M, Lichtman I D, Davies A G, Thorne P D, Bass S J. 2015. Sticky stuff: Redefining bedform prediction in modern and ancient environments. Geology, 43: 399–402
Wang J, Liu P, Gao Z R, Bai S B, Cao G J, Qu G X. 2007. Temporal-spatial variation of the channel in Jiangsu reach of the Yangtze River during the last 44 years (in Chinese). Acta Geol Sin, 11: 1185–1193
Wang W W, Fan F X, Li C G, Yan J. 2007. Activity of submarine sand waves and seafloor erosion and deposition in the sea area to the southwest of Hainan Island (in Chinese). Mar Geol Quat Geol, 27: 23–28
Wang Z, Chen Z Y, Shi Y F, Li M T, Zhang Q, Wei T Y. 2007. The fluvial bedform and hydrodynamic controls along the middle and lower Yangtze River (from Wuhan to estuary) (in Chinese). Sci China Ser D-Earth Sci, 37: 1223–1234
Wu J, Wang Y, Cheng H. 2009. Bedforms and bed material transport pathways in the Changjiang (Yangtze) Estuary. Geomorphology, 104: 175–184
Wu S H, Cheng H Q, Li J F, Zheng S W. 2016. Recent morphological variation and micro-topography features in North Channel of the Yangtze Estuary (in Chinese). J Sediment Res, 2: 26–32
Wu Z Y, Li J B, Jin X L, Shang J H, Li S J, Jin X B. 2014. Distribution, features, and influence factors of the submarine topographic boundaries of the Okinawa Trough. Sci China Earth Sci, 57: 1885–1896
Wu Z Y, Saito Y, Zhao D N, Zhou J Q, Cao Z Y, Li S J, Shang J H, Liang Y Y. 2016. Impact of human activities on subaqueous topographic change in Lingding Bay of the Pearl River estuary, China, during 1955–2013. Sci Rep, 6: 37742
Xia J Q, Deng S S, Lu J Y, Xu Q X, Zong Q L, Tan G M. 2016. Dynamic channel adjustments in the Jingjiang Reach of the Middle Yangtze River. Sci Rep, 6: 22802
Xu Q X. 2013. Study of sediment deposition and erosion patterns in the middle and downstream Changjiang mainstream after impoundment of TGR (in Chinese). J Hydroel Eng, 2: 146–154
Yang S L, Milliman J D, Li P, Xu K. 2011. 50000 dams later: Erosion of the Yangtze River and its delta. Glob Planet Change, 75: 14–20

Yang S L, Milliman J D, Xu K H, Deng B, Zhang X Y, Luo X X. 2014. Downstream sedimentary and geomorphic impacts of the Three Gorges Dam on the Yangtze River. Earth-Sci Rev, 138: 469–486

Yang S L, Xu K H, Milliman J D, Yang H F, Wu C S. 2015. Decline of Yangtze River water and sediment discharge: Impact from natural and anthropogenic changes. Sci Rep, 5: 12581

Zhong D Y, Wang Q X, Ding Y. 2005. Influence of sand wave migration on non-saturated suspended load transport in alluvial rivers (in Chinese). J Hydraul Engineering, 36: 1432–1438

Zheng S W, Cheng H Q, Wu S H, Liu G W, Lu X J, Xu W X. 2016. Discovery and implications of catenary-bead subaqueous dunes. Sci China Earth Sci, 59: 495–502

Zheng S W, Cheng H Q, Wu S H, Shi S Y, Xu W, Zhou Q P, Jiang Y H. 2017. Morphology and mechanism of the very large dunes in the tidal reach of the Yangtze River, China. Cont Shelf Res, 139: 54–61

Zhuang Z Y, Lin Z H, Zhou J, Liu Z F, Liu Y F. 2004. Environmental conditions for the formation and development of sand dunes (waves) in the continental shelf (in Chinese). Mar Geol Lett, 20: 5–10

(Responsible editor: Chansheng HE)